

Supplementary Materials for

Discovery of natural MgSiO_3 tetragonal garnet in a shocked chondritic meteorite

Naotaka Tomioka, Masaaki Miyahara, Motoo Ito

Published 25 March 2016, *Sci. Adv.* **2**, e1501725 (2016)

DOI: 10.1126/sciadv.1501725

The PDF file includes:

Fig. S1. Pressure-temperature phase diagram of MgSiO_3 .

Fig. S2. Polarized optical micrographs of a fragment of host rock captured in a shock vein.

Fig. S3. Raman spectrum of majorite at the rim of a shock vein in Tenham.

Fig. S4. Transmission electron micrograph of the entire ultrathin foil sample of a tetragonal majorite aggregate processed by an FIB.

Fig. S5. Schematic diagrams of electron diffraction patterns of cubic ($Ia\bar{3}d$) and tetragonal ($I4_1/a$) majorites along the $\langle 001 \rangle$ and $\langle 010 \rangle$ zone axes.

Fig. S6. One- and two-dimensional electron diffraction profiles of natural and synthetic majorites.

Fig. S7. One-dimensional thermal conductivity model used for estimating the temperature paths of a shock vein cooled by the host rock of a meteorite.

Table S1. Chemical composition of $(\text{Mg,Fe})\text{SiO}_3$ tetragonal majorite.

Supplementary Materials

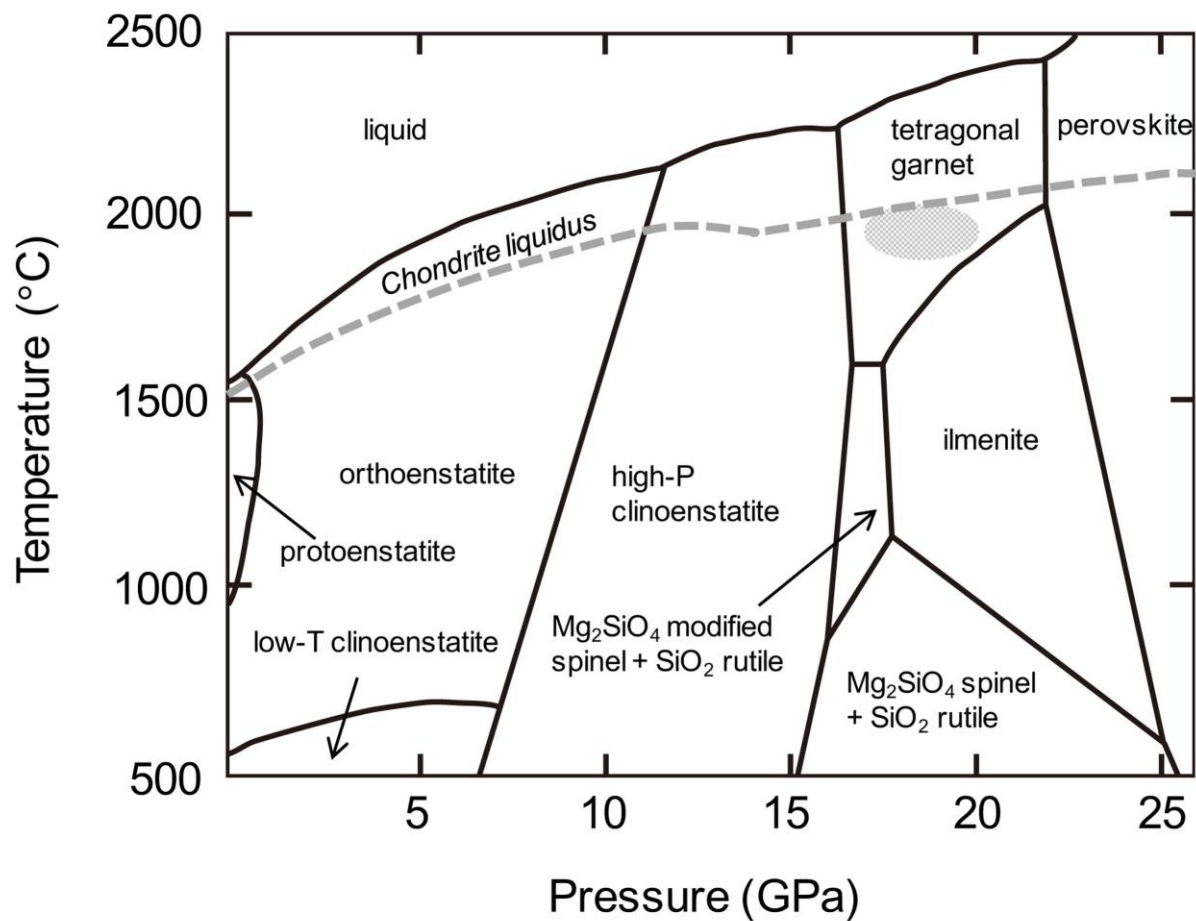


fig. S1. Pressure-temperature phase diagram of MgSiO₃ [modified from (19)]. Pyroxene (enstatite) transforms into the tetragonal garnet phase, ilmenite phase, and perovskite phase with increasing pressure at high temperature. The broken line indicates the liquidus curve of bulk chondrites (37). The shaded area represents the estimated pressure-temperature conditions of the formation of (Mg,Fe)SiO₃ tetragonal majorite in Tenham.

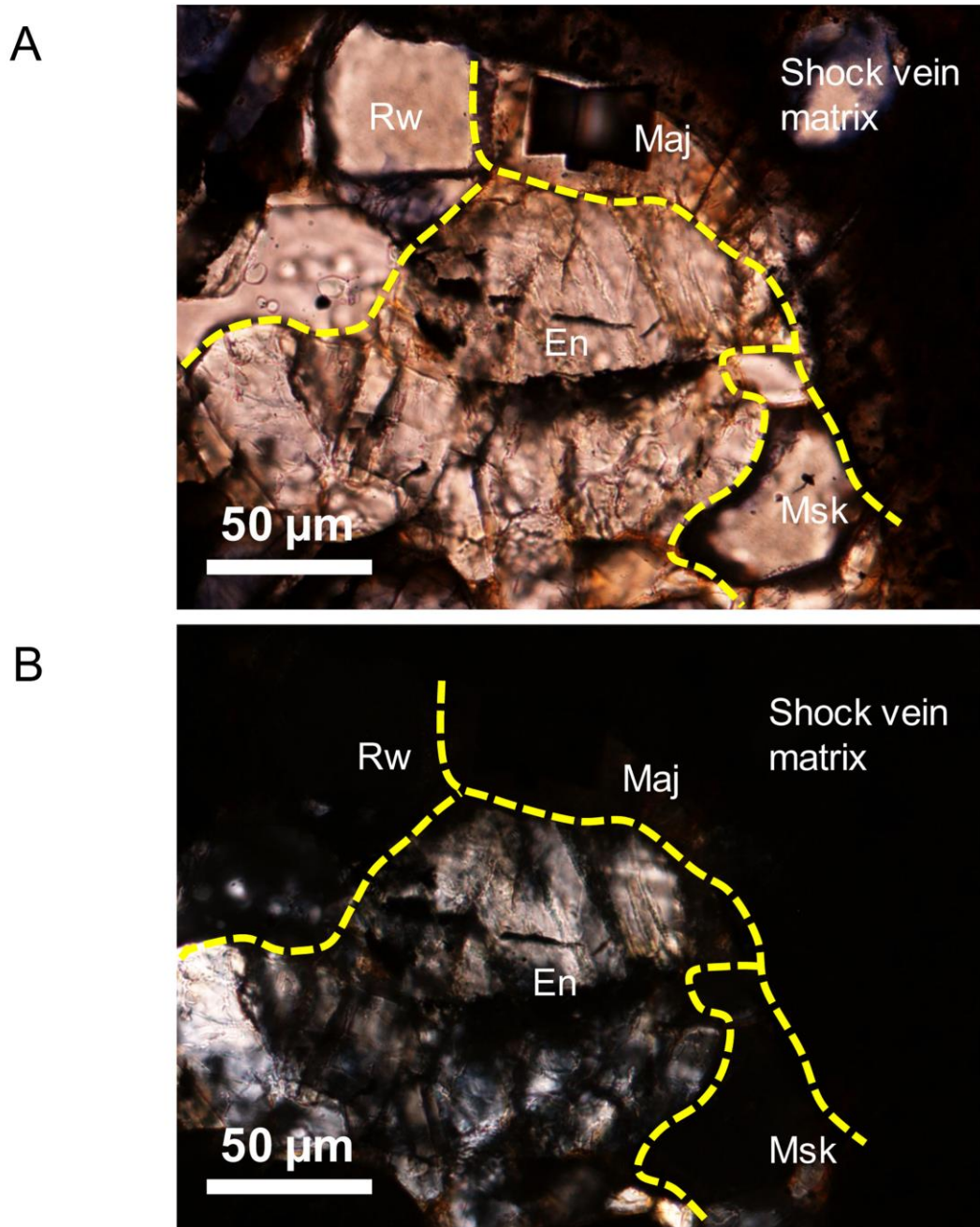


fig. S2. Polarized optical micrographs of a fragment of host rock captured in a shock vein. Maj: $(\text{Mg,Fe})\text{SiO}_3$ majorite, Rw: $(\text{Mg,Fe})_2\text{SiO}_4$ spinel (ringwoodite), and En: $(\text{Mg,Fe})\text{SiO}_3$ pyroxene. (A) Open Nicol image; (B) crossed Nicols image. The portion of majorite is seemingly optically isotropic owing to very small tetragonal distortion from cubic symmetry. The surface of the left part of the majorite aggregate was processed to be an ultrathin foil by a focused ion beam (FIB).

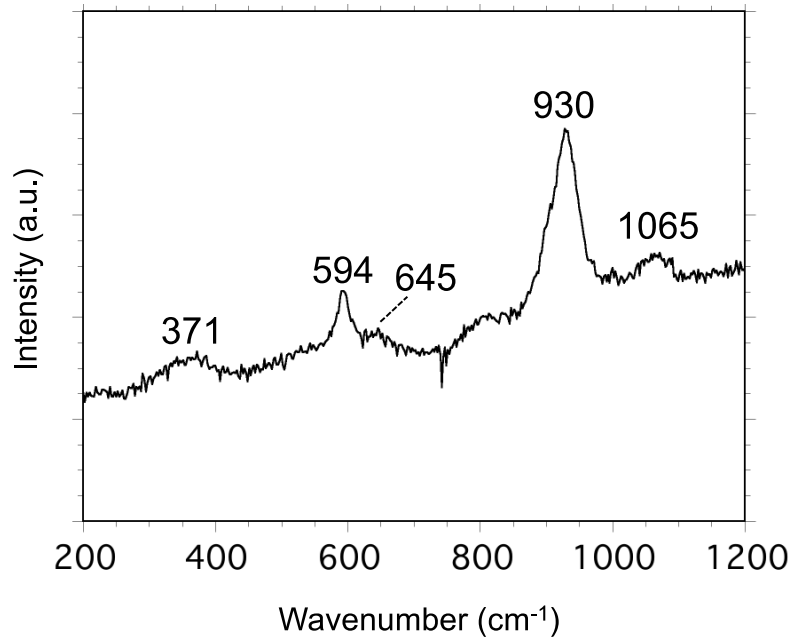


fig. S3. Raman spectrum of majorite at the rim of a shock vein in Tenham. The Raman measurements were performed using a micro-Raman spectrometer system. An argon laser with a wavelength of 514.5 nm (Jobin Yvon T64000) at Kochi University was focused to spot size of 2 μm with a laser power of 5 mW on the desired portion of the polished thin section.

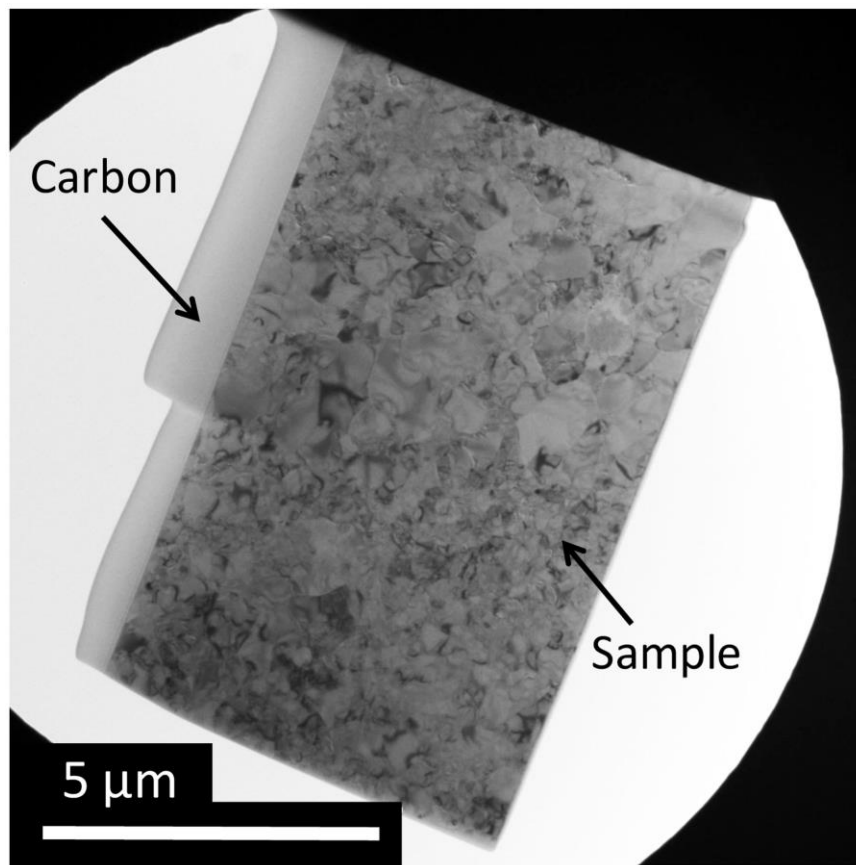


fig. S4. Transmission electron micrograph of the entire ultrathin foil sample of tetragonal majorite aggregate processed by an FIB. A carbon layer was deposited to protect the sample in FIB fabrication.

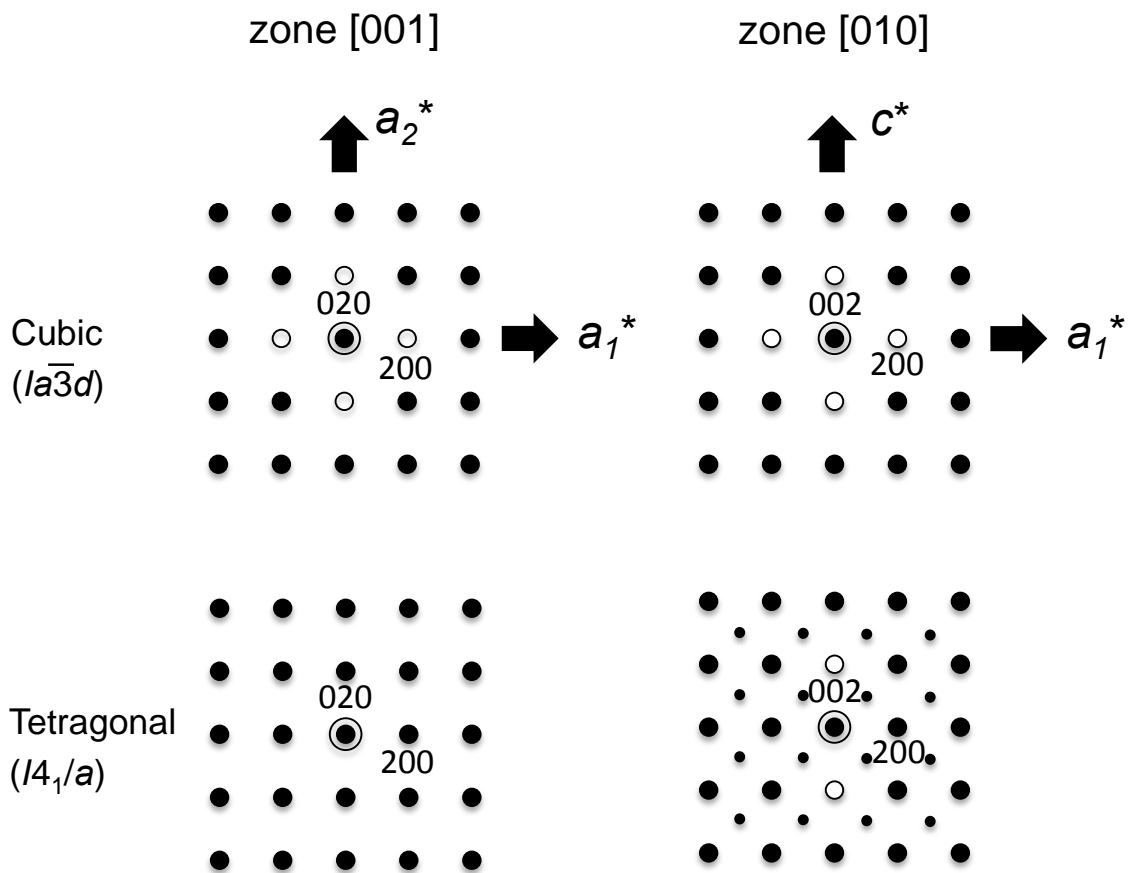


fig. S5. Schematic diagrams of electron diffraction patterns of cubic ($Ia\bar{3}d$) and tetragonal ($I4_1/a$) majorites along the $\langle 001 \rangle$ and $\langle 010 \rangle$ zone axes. Diffraction spots shown by open circles violate the extinction rules in Bragg diffraction, but can appear due to the multiple diffractions. The $I4_1/a$ symmetry can be diagnosed by the presence of $\{h0l\}$ reflections with h and l both of which are odd, as shown by small filled circles.

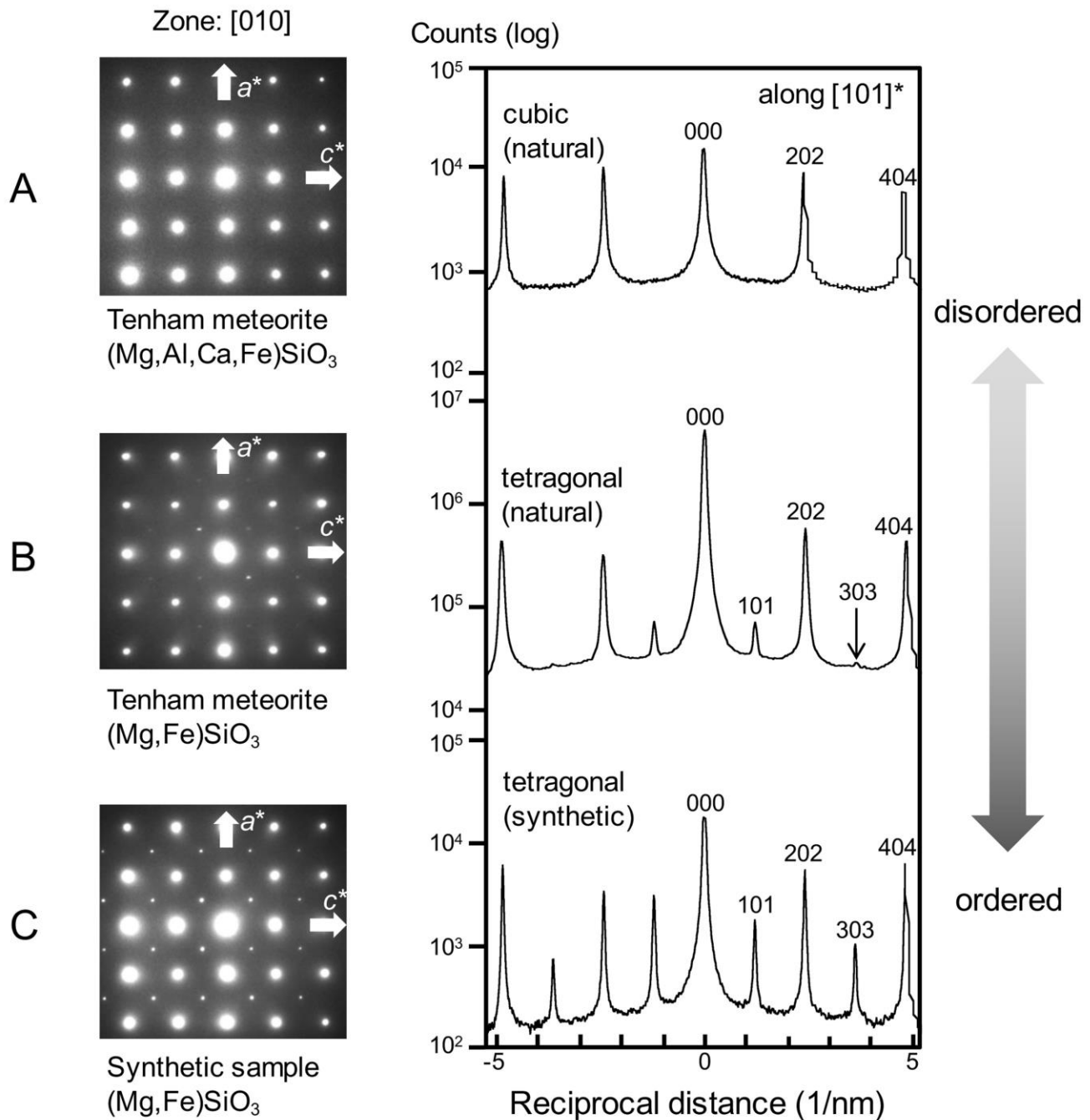


fig. S6. One- and two-dimensional electron diffraction profiles of natural and synthetic majorites. One-dimensional profiles were taken along the $[101]^*$ direction. (A) Al- and Ca-rich $(\text{Mg,Fe})\text{SiO}_3$ majorite [Al_2O_3 : 4.6 wt%; CaO : 2.1 wt% (16)] crystallized from shock-induced chondritic melt in Tenham. (B) $(\text{Mg,Fe})\text{SiO}_3$ majorite formed in a solid-state transformation of low-Ca pyroxene in Tenham. (C) Synthetic $(\text{Mg,Fe})\text{SiO}_3$ majorite synthesized at 20 GPa and 2200 °C by Kawai-type high pressure apparatus by (28). Al- and Ca-rich $(\text{Mg,Fe})\text{SiO}_3$ majorite showing cubic symmetry.

By way of contrast, both natural and synthetic (Mg,Fe)SiO₃ majorite show a tetragonal symmetry with diagnostic reflections for the space group $I4_1/a$ ($\{h0l\}$: both h and l are odd). However, the intensities of $\{h0l\}$ reflections with h and l both of which are odd in natural (Mg,Fe)SiO₃ majorite are significantly weaker than those of the synthetic sample. The difference in diffraction intensities was caused by the different degree of ordering of Mg, Fe, and Si in octahedral sites in its crystal structure.

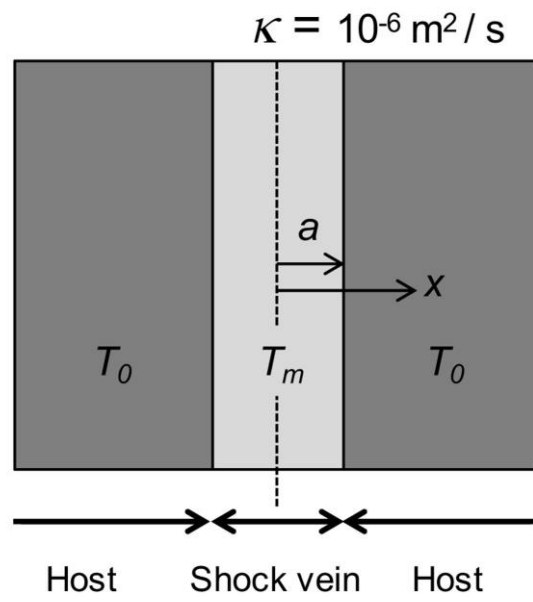


fig. S7. One-dimensional thermal conductivity model used for estimating the temperature paths of a shock vein cooled by the host rock of a meteorite.

table S1. Chemical composition of (Mg,Fe)SiO₃ tetragonal majorite.

Constituent	Wt %	Range	Stand. Dev.
Na ₂ O	n.d.	---	---
MgO	28.91	28.00–29.73	0.49
Al ₂ O ₃	0.20	0.06–0.25	0.05
SiO ₂	56.39	55.62–57.16	0.48
CaO	0.91	0.84–1.07	0.06
TiO ₂	0.20	0.17–0.25	0.02
Cr ₂ O ₃	0.14	0.10–0.19	0.03
MnO	0.72	0.63–0.82	0.05
FeO	12.46	11.92–13.18	0.28
Total	100*		

*In thin foil (100 nm in thickness) analyses using an energy dispersive X-ray spectrometer equipped with a transmission electron microscope, the total weight percentage is normalized to 100%.